

Dynamic scaling in surface-controlled colloidal aggregation

This article has been downloaded from IOPscience. Please scroll down to see the full text article.

2000 J. Phys.: Condens. Matter 12 A281

(<http://iopscience.iop.org/0953-8984/12/8A/336>)

View [the table of contents for this issue](#), or go to the [journal homepage](#) for more

Download details:

IP Address: 129.252.86.83

The article was downloaded on 27/05/2010 at 11:27

Please note that [terms and conditions apply](#).

Dynamic scaling in surface-controlled colloidal aggregation

A Schmitt[†], A Fernández-Barbero[‡], M A Cabrerizo-Vílchez[†] and
R Hidalgo-Álvarez[†]

[†] Biocolloid and Fluid Physics Group, Department of Applied Physics, University of Granada,
Campus de Fuentenueva, E-18071 Granada, Spain

[‡] Complex Fluid Physics Group, Department of Applied Physics, University of Almería, Cañada
de San Urbano s/n, E-04120 Almería, Spain

Received 12 August 1999

Abstract. In this work, the aggregation behaviour of surface-modified colloidal particles was studied. In view of this, a method was developed which allows the dynamic scaling functions $s(t)$ and $\Phi(x)$ to be calculated from single-cluster light scattering data. The method was employed to investigate the aggregation of colloidal particles covered with different amounts of bovine serum albumin (BSA). It was found that BSA molecules do not alter the aggregation regime when the samples aggregate at the protein's isoelectric point. Far from this condition, however, the adsorbed protein molecules increase the residual electrostatic interaction and the aggregation regime changes from diffusion- to reaction-controlled aggregation.

1. Introduction

Over the last few years, scaling concepts have been very successfully used to describe growth and structure formation phenomena. Especially in the field of colloidal science, spatial and temporal scaling proved to be an excellent tool for analysing colloidal aggregation phenomena.

The dynamic scaling properties can be obtained directly from the complete cluster-size distributions. Experimental techniques, however, resolve only a limited number of cluster sizes or register some average mean cluster size. This makes it difficult to extract the dynamic scaling properties from experimental data. In the first part of this paper, we develop a novel fitting procedure which allows the dynamic scaling functions to be calculated directly from single-cluster light scattering data.

In the second part, this method is used to study the aggregation behaviour of colloidal particles coated with different amounts of adsorbed macromolecules. This type of aggregation phenomenon plays an important role in many industrial applications such as food preparation, waste water treatment, etc. In this study, bovine serum albumin (BSA) will be adsorbed onto the particle surface. The net charge of the BSA molecules and hence the surface charge of BSA-covered particles depends strongly on the pH of the aqueous phase. Furthermore, additional short-range effects like interparticle bridging and steric stabilization come into play depending on the degree of surface coverage. This means that the adsorbed protein molecules allow one to change the particle surface characteristics quite drastically and, thus, the question of to what extent the particle surface characteristics alter the aggregation behaviour of colloidal suspensions may be studied.

2. Theoretical background

In dilute systems, colloidal aggregation is described by von Smoluchowski’s equation [1]:

$$\frac{dc_n}{dt} = \frac{1}{2} \sum_{i+j=n} k_{ij}c_i c_j - c_n \sum_{i=1}^{\infty} k_{ni}c_i. \tag{1}$$

Here, $c_n(t)$ denotes the number concentration of aggregates of size n (n -mers). The set of parameters k_{ij} is the concentration-independent aggregation kernel which quantifies the rate at which i -mers and j -mers react to form aggregates of size $i + j$. The aggregation kernel, k_{ij} , contains the physical information about the aggregation process. Equation (1) takes into consideration only binary collisions which generate or deplete a given cluster size n . The first term on the right-hand side corresponds to the rate at which n -mers are formed when i -mers react with $(n - i)$ -mers. The second term on the right-hand side quantifies the loss of n -mers due to binary reactions with other aggregates.

Van Dongen and Ernst developed the following classification scheme for homogeneous kernels in terms of the scaling exponents λ and μ [2, 3]:

$$\begin{aligned} k_{(ai)(aj)} &\approx a^\lambda k_{ij} & \lambda &\leq 2 \\ k_{i \ll j} &\approx k_0 i^\mu j^\nu & \nu &= (\lambda - \mu) \leq 1 \end{aligned} \tag{2}$$

where a is a large positive constant and k_0 a scale factor. The homogeneity exponents λ become zero for diffusion-limited aggregation [4]. For reaction-limited aggregation, however, values of $\lambda \approx 0.5$ and $\lambda \approx 1$ are reported in the literature [4, 5].

For systems which do not give rise to gel formation ($\lambda \leq 1$), the cluster-size distribution can be expressed as [2]

$$c_n(t) \sim s^{-2} \Phi(n/s). \tag{3}$$

$\Phi(x)$ may be understood as a time-independent scaling distribution. The time-dependent scaling function, $s(t)$, is related to some average mean cluster size. It should be pointed out that equation (3) is strictly valid only for large aggregates and long times. Recent investigations, however, confirmed that systems aggregating from monomeric initial conditions reach the dynamic scaling limit even for small aggregates and at relatively short times [6, 7].

For non-gelling kernels, the scaling function $s(t)$ is given by [5]

$$s(t) = \begin{cases} [C_1 + (1 - \lambda)C_2 t]^{1/(1-\lambda)} & \lambda < 1 \\ C_1 \exp(C_2 t) & \lambda = 1 \end{cases} \tag{4}$$

where C_1 and C_2 are constants. At sufficiently long times, $s(t)$ grows as a power law in time when $\lambda < 1$:

$$\lim_{t \rightarrow \infty} s(t) \sim t^{1/(1-\lambda)}. \tag{5}$$

Under some special conditions, the exact relationship between $s(t)$ and the number-average mean cluster size, $\langle n_n \rangle$, is known explicitly and is given by [5]

$$s(t) \sim \begin{cases} \langle n_n \rangle & \tau < 1 \text{ or } \mu < 0 \\ \langle n_n \rangle^{1/(2-\tau)} & 1 < \tau < 2 \end{cases} \tag{6}$$

where τ is a scaling exponent which characterizes the long-time behaviour of the cluster-size distribution. For diffusion-limited aggregation, $s(t)$ is directly proportional to $\langle n_n \rangle$. For other aggregation regimes, however, the exact relationship is not known *a priori* since the exact value of τ must be determined first.

3. Materials and methods

3.1. Experimental system

Two aqueous suspensions of spherical polystyrene particles were employed for the aggregation experiments. The two systems have very similar characteristics, i.e. they are charge stabilized by sulphate groups, have diameters of approximately 600 nm and are highly monodisperse. The only significant difference lies in the particle surface charge density. Conductimetric titration showed that the surface charge density of $(-76 \pm 4) \text{ mC m}^{-2}$, obtained for sample AS2, is about three times that of $(-24 \pm 1) \text{ mC m}^{-2}$, measured for sample AS8.

The particle surface was modified by the adsorbing of different amounts of bovine serum albumin (BSA). Particles with five different degrees of surface coverage, θ , were prepared. The values selected for θ were 0%, 25%, 50%, 75% and 100%. The uncovered particles ($\theta = 0\%$) were treated in exactly the same way as all other samples. The only difference was that no protein was added.

Two series of aggregation experiments were carried out, one at pH 5 and one at pH 9. The pH was maintained at 5.0 by means of an acetate buffer and at pH 9.0 by means of a borate buffer. The electrolyte concentration and initial particle concentration were 1.0 M KCl and $1.0 \times 10^{14} \text{ m}^{-3}$, respectively. The temperature was stabilized at 21 °C.

3.2. The single-cluster light scattering instrument

Single-cluster light scattering (SCLS) was employed to monitor the cluster-size distribution during aggregation. The instrument used for this study counts the total number of particles and classifies aggregates up to heptamers according to their size. This makes it possible to calculate the number-average mean cluster size as $\langle n_n \rangle(t) = c_0 / \sum_{n=1}^{\infty} c_n(t)$ where c_0 is the initial particle concentration and $\sum_{n=1}^{\infty} c_n(t)$ the overall number concentration of aggregates. Higher-order averages, such the weight-average mean cluster size, $\langle n_w \rangle$, or the z -average mean cluster size, $\langle n_z \rangle$, cannot be detected since they require a more detailed knowledge of the complete cluster-size distribution. The initial aggregation rate constant, k_{11} , can be obtained from the time evolution of the monomer concentration. For a more detailed description of the light scattering set-up and data treatment, see [7, 8].

4. Results and discussion

The results section is divided into two parts. In the first part, a novel fitting procedure will be developed which allows us to extract the dynamic scaling properties from experimental cluster-size distributions as obtained by SCLS. In the second part, the method will be used to study the influence of the particle surface characteristics on the dynamic scaling properties of aggregating colloidal particles.

4.1. Experimental determination of the dynamic scaling properties

As mentioned above, the scaling function $s(t)$ is related to some average mean cluster size. Due to the limitations of the SCLS instrument, $s(t)$ has to be expressed in terms of the number-average mean cluster size, $\langle n_n \rangle$, since other average cluster sizes are not experimentally accessible.

Equation (6) suggests a power-law dependence between $s(t)$ and $\langle n_n \rangle$:

$$s(t) \sim \langle n \rangle^\alpha \quad (7)$$

where $\alpha \geq 1$.

The dynamic scaling distribution $\Phi(x)$ can now be calculated according to equation (3) using α as a fitting parameter. The best fit is obtained when the different curves, $c_n(t)$, of the cluster-size distribution collapse and define one single master curve.

Combining equation (5) with equation (7) yields

$$\langle n_n \rangle \sim t^{1/(\alpha(1-\lambda))} \tag{8}$$

which indicates that the number-average mean cluster size grows as a power of time according to

$$\langle n_n \rangle \sim t^w \tag{9}$$

where $w = 1/[\alpha(1 - \lambda)]$. Solving for λ finally gives

$$\lambda = 1 - \frac{1}{\alpha w}. \tag{10}$$

Thus, λ may be calculated from the long-time behaviour of $\langle n_n \rangle$ once the fitting parameter α is known.

Figure 1 shows an example of the fitting method described for the completely covered particles AS8 aggregating at pH 5. The plot in the lower left-hand corner shows the dynamic scaling distribution $\Phi(x)$ calculated for $\alpha = 1$. In this case, the different curves corresponding to monomers, dimers, trimers etc are clearly distinguishable and no single master curve is found. The main plot shows the same data calculated for $\alpha = 2.3$. Only in this case do the different curves collapse and define the time-independent scaling distribution $\Phi(x)$ correctly.

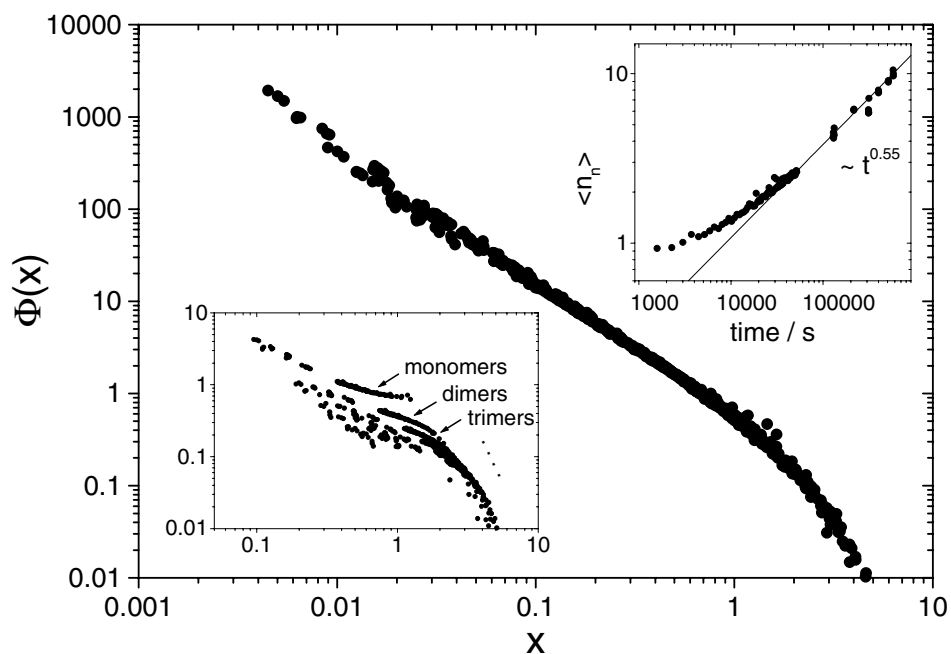


Figure 1. The dynamic scaling distribution $\Phi(x)$ for completely covered particles AS8 aggregating at pH 5. The dynamic scaling distribution was calculated for $\alpha = 2.3$. The plot in the lower left-hand corner shows the same data for $\alpha = 1$. The time evolution of the number-average cluster size $\langle n_n \rangle$ is plotted in the upper right-hand corner.

The plot in the upper right-hand corner of figure 1 shows the time evolution of the number-average cluster size $\langle n_n \rangle$. An asymptotic behaviour according to equation (9) can be observed. The best fit for the exponent w yields 0.55 ± 0.06 . Using this result in equation (10) gives finally for the homogeneity exponent $\lambda = 0.21 \pm 0.16$.

4.2. Experimental results

Two series of aggregation experiments at high electrolyte concentration were carried out as functions of the particle surface coverage. At high salt concentration, the particle surface charge is almost completely screened and only some small residual electrostatic interactions may remain [6], so the uncovered samples are expected to aggregate in the diffusion-limited aggregation regime. For particles with intermediate and high degrees of surface coverage, bridging flocculation and steric stabilization should be observed.

The first series of aggregation experiments correspond to samples AS8 and AS2 at pH 5. Under this condition, the BSA molecules are at their isoelectric point and no additional electric net charge is introduced by the presence of adsorbed BSA molecules. Consequently, the repulsive electrostatic interactions between the particles remain almost unaltered.

Table 1 contains the initial rate constants k_{11} obtained for different degrees of surface coverage. As expected, the aggregation rates for the uncovered particles agree perfectly with the rate of $(6 \pm 3) \times 10^{-12} \text{ cm}^3 \text{ s}^{-1}$ commonly reported for diffusion-limited aggregation [9]. The values obtained for the scaling exponent λ confirm this finding. As can be seen in table 2, λ is, within its experimental error, always close to zero for bare particles.

Table 1. Initial rate constants k_{11} ($10^{-12} \text{ cm}^3 \text{ s}^{-1}$).

pH	Sample	Degree of surface coverage				
		0%	25%	50%	75%	100%
5.0	AS8	7.3 ± 1.8	6.2 ± 1.5	5.8 ± 1.4	3.6 ± 0.9	1.5 ± 0.4
	AS2	8.2 ± 2.0	7.0 ± 1.7	5.6 ± 1.4	3.1 ± 0.8	5.2 ± 1.3
9.0	AS8	7.3 ± 1.8	6.2 ± 1.5	2.5 ± 0.6	1.8 ± 0.4	0.8 ± 0.2
	AS2	6.2 ± 1.6	5.6 ± 1.4	3.2 ± 0.8	0.09 ± 0.02	0.06 ± 0.02

Table 2. Homogeneity exponent λ .

pH	Sample	Degree of surface coverage				
		0%	25%	50%	75%	100%
5.0	AS8	0.09 ± 0.18	0.07 ± 0.18	0.04 ± 0.19	0.05 ± 0.19	0.21 ± 0.16
	AS2	0.17 ± 0.17	0.09 ± 0.18	0.17 ± 0.17	0.17 ± 0.17	0.04 ± 0.19
9.0	AS8	0.09 ± 0.18	-0.01 ± 0.20	0.17 ± 0.17	0.38 ± 0.12	0.27 ± 0.14
	AS2	0.17 ± 0.17	0.04 ± 0.19	0.11 ± 0.18	(0.72 ± 0.06)	(0.93 ± 0.01)

At intermediate and high degrees of surface coverage, k_{11} decreases gradually by a factor of approximately three or four. This suggests that the particle aggregation mechanism is drifting away from the diffusion-limited aggregation regime. Nevertheless, the scaling exponent λ remains practically zero and, hence, does not confirm this hypothesis. This indicates that particle diffusion is still the predominant aggregation factor although more than one interparticle collision becomes necessary for the formation of a stable bond.

The second series of aggregation experiments was carried out at pH 9 where the adsorbed BSA molecules bear negative net charge. Here, the adsorbed BSA molecules increment the surface charge of the particles and, thus, alter the repulsive electrostatic interactions. This implies that the effect of residual interactions should be stronger, so bridging flocculation should become more difficult and the effect of steric stabilization enhanced.

The experimental results confirm this hypothesis. For the uncovered particles, k_{11} and λ are very similar to the results obtained at pH 5. This means that the uncovered particles are still aggregating in the diffusion-limited aggregation regime. At intermediate and high degrees of surface coverage, however, a significant decrease is observed for the aggregation rate k_{11} . For the samples with 50% surface coverage, the aggregation rate drops for both samples by a factor of approximately two. Nevertheless, λ remains very close to zero, so the whole aggregation process is still controlled by the diffusive motion of the aggregates. At higher degrees of surface coverage, the aggregation rate decreases by a factor of 10 for sample AS8 and by a factor of 100 for sample AS2. Hence, about 10 to 100 diffusive collisions are needed for completely covered particles before a stable bond can be formed. It becomes evident that the aggregation process cannot be diffusion controlled any longer. The values measured for λ confirm this finding. For sample AS8, λ rises to about 0.4 while for sample AS2 a value of 0.9 is reached, indicating that the samples entered the slow aggregation regime. Nevertheless, it is not clear whether the limiting value for λ should be 0.5 or 1 since the data for sample AS2 should be treated with caution. The aggregation rates for the highly covered particles AS2 are so low that it is not clear whether dynamic scaling is already completely developed. This is why the corresponding values for λ are reported in brackets. Nevertheless, the data confirm the tendency observed for the system AS8. The correct value for λ in the slow-colloidal-aggregation regime remains, however, an open question. Nevertheless, it becomes clear that the particle surface characteristics are of paramount importance for the aggregation behaviour of colloidal suspensions, and the experimental results presented in this work may help us to gain further insight into short-range interactions mediated by adsorbed protein molecules.

Acknowledgments

This work was supported by the CICYT (Project MAT97-1024). AS is grateful for a scholarship granted by the Gottlieb Daimler- and Karl Benz-Stiftung

References

- [1] von Smoluchowski M 1917 *Z. Phys. Chem.* **92** 129
- [2] van Dongen P G J and Ernst M H 1985 *Phys. Rev. Lett.* **54** 1396
- [3] van Dongen P G J and Ernst M H 1988 *J. Stat. Phys.* **50** 295
- [4] Ball R C, Weitz T A, Witten T A and Leyvraz F 1987 *Phys. Rev. E* **58** 274
- [5] Broide M L and Cohen R J 1992 *J. Colloid Interface Sci.* **153** 493
- [6] Fernández-Barbero A, Cabrerizo-Vílchez M A, Martínez-García R and Hidalgo-Álvarez R 1996 *Phys. Rev. E* **53** 4981
- [7] Fernández-Barbero A, Schmitt A, Cabrerizo-Vílchez M A and Martínez-García R 1996 *Physica A* **230** 53
- [8] Holthoff H, Schmitt A, Fernández-Barbero A, Borkovec M, Cabrerizo-Vílchez M A, Schurtenberger P and Hidalgo-Álvarez R 1997 *J. Colloid Interface Sci.* **192** 463
- [9] Sonntag H and Strenge K 1987 *Coagulation Kinetics and Structure Formation* (New York: Plenum)